



Revisiting generalized synchronization: Progress and perspectives

H. H. JAFRI¹, TH. UMESHKANTA SINGH² and K. MANCHANDA^{3,*}

¹Department of Physics, Aligarh Muslim University, Aligarh 202 002, India

²Department of Physics, Shivaji College, University of Delhi, New Delhi 110 027, India

³School of Arts and Sciences, Azim Premji University, Bengaluru 562 125, India

*Corresponding author. E-mail: kaustubh.manchanda@apu.edu.in

Abstract. ‘Generalized synchronization (GS)’ was proposed by Rulkov *et al.* (*Phys. Rev. E* **51**, 980 (1995)) to explain synchronization in unidirectionally coupled systems. This concept has been effective in providing a deeper understanding of synchronization between several non-identical nonlinear systems. The study of GS has been extended to various coupling schemes ranging from bidirectionally coupled systems to complex networks. We review the major ideas that were involved in the field of GS. The characterizing tools to detect generalized synchrony and its types along with their relative merits are discussed. We outline some of the interesting results that were published in the last two decades along with the inter-relatedness of different dynamical phenomena reported in coupled dynamical systems.

Keywords. Chaotic systems; generalized synchronization; complex networks.

PACS Nos 05.45.–a; 05.45.+b; 05.45.Xt; 05.45.Ac; 89.75.Hc; 43.72.+q; 47.52.+j

1. Introduction

Isolated dynamical systems are rare in nature since systems either interact with each other or with an environment [1–6]. Depending on the nature of interaction, several coupling schemes can be found in the literature [7]. When one dynamical system is driven by another (unidirectional), the latter being unaffected by the former, this setting is called the drive–response configuration, while a mutual interaction leads to a bidirectional coupling.

Interactions between dynamical systems can lead to a plethora of possibilities in terms of dynamical phenomena. Amongst the various possible outcomes, temporal correlation also referred to as synchronization [8, 9] is the most fundamental and ubiquitous [10–13] in nature. A standard way to define it is as follows: Synchronization is the adjustment of rhythms of oscillating objects due to their weak interaction [14]. In the earlier days, nonlinear-dynamical systems with extreme sensitivity to initial conditions seemed to defy the phenomenon of synchronization which is otherwise universal in nature. Starting in 1983, Fujisaka and Yamada [15] published several papers on the stability of synchronized motion of coupled-chaotic oscillators by considering several aspects of symmetrical couplings, and they developed a

stability theory based on the Lyapunov matrix. In 1990, Pecora and Carroll’s classical paper on synchronization in chaotic systems [16] described how two chaotic subsystems could be synchronized by linking them with a common signal. Since then chaos synchronization has emerged as a highly active interdisciplinary area of research in the field of nonlinear science.

Depending on the type of coupling and nature of the system, different regimes of synchrony arise, namely, (1) complete synchronization (CS) [16], (2) lag synchronization (LS) [17], (3) phase synchronization [18] and (4) generalized synchronization (GS). Different studies investigating the order in which these synchronies arise in different dynamical systems and their relative strengths can be found in [17, 19–22]. This work is dedicated to the study of GS. We review the works of all the key contributors in the field, right from its inception to the important theoretical developments, industry applications and discuss the prospects for future research in the domain of GS.

The presence of GS has been established in several theoretical scenarios such as unidirectionally coupled partial differential equations [23], discrete coupled maps [24] and flows [25] as well as in various experimental settings [26], namely electronic circuits [27], laser systems [28, 29], chemical systems [30], chaotic

communication [31, 32], chaotic switching schemes [33] and so on, thereby highlighting the ubiquity of the phenomenon and hence the importance of this work.

This review is organized as follows: Works related to emergence of GS in different settings are summarized in section 2. This is followed by a study on detection techniques of GS in section 3. Types of GS and the tools to discern the transition between different regimes of generalized synchrony are discussed in section 4. Section 5 focuses on the emergence of GS in complex networks. Experimental detection and practical applications of GS form the subject of section 6. Future outlook is explored in section 7. The work concludes with a summary and discussion in section 8.

2. Generalized synchronization

In coupled dynamical systems, the most general and probably the most universal form of temporal correlation is GS. When the nature of interaction between two dynamical systems is unidirectional, one being the drive and the other being the response, then if the response signal is uniquely dependent on the drive, the two are said to be in generalized synchrony. In this drive–response configuration, if the evolution equations of the drive and response are given by

$$\begin{aligned}\dot{\mathbf{x}} &= F(\mathbf{x}), \\ \dot{\mathbf{y}} &= G(\mathbf{x}, \mathbf{y}),\end{aligned}\quad (1)$$

respectively, then the onset of GS can be identified by the stabilization of the dynamics of the response by the drive. Here $\mathbf{x} \in \mathbb{R}^n$ and $\mathbf{y} \in \mathbb{R}^m$ are the dynamical variables of the drive and response, respectively. F and G are continuous-nonlinear functions governing the evolution of dynamical variables.

As an example, we consider two different chaotic systems: Magneto-hydrodynamics system and Lorenz model [34]. The set of equations for the magneto-hydrodynamics system is given by

$$\begin{aligned}\frac{dx_1}{dt} &= a_1(x_2 - x_1), \\ \frac{dx_2}{dt} &= x_1x_3 - x_2, \\ \frac{dx_3}{dt} &= b_1 - x_1x_2 - c_1x_3,\end{aligned}\quad (2)$$

where $a_1 = 5$, $b_1 = 14.625$ and $c_1 = 1$. Equations for the Lorenz system are:

$$\frac{dy_1}{dt} = a_2(y_2 - y_1),$$

$$\begin{aligned}\frac{dy_2}{dt} &= b_2y_1 - y_2 - y_1y_3, \\ \frac{dy_3}{dt} &= y_1y_2 - c_2y_3,\end{aligned}\quad (3)$$

where $a_2 = 10$, $b_2 = 28$ and $c_2 = 8/3$.

To introduce an interaction between the two systems (eqs (2) and (3)), we consider the Pecora–Carroll’s coupling scheme [16], namely the magneto-hydrodynamics system is taken as the drive while the Lorenz system acts as the response. The equations of the drive and response systems (after coupling) are given below.

$$\begin{aligned}\frac{dx_1}{dt} &= a_1(x_2 - x_1), & \frac{dy_1}{dt} &= a_2(x_2 - y_1), \\ \frac{dx_2}{dt} &= x_1x_3 - x_2, \\ \frac{dx_3}{dt} &= b_1 - x_1x_2 - c_1x_3, & \frac{dy_3}{dt} &= y_1x_2 - c_2y_3.\end{aligned}\quad (4)$$

Here, the coupling is achieved through the x_2 variable of the drive system, namely the drive sends the x_2 signal to the response, which has its y_2 variable missing.

Figure 1 shows the attractors and the trajectories of the drive–response system. In figure 1a the attractor of the magneto-hydrodynamics (drive) system is shown in red colour. Before the onset of coupling, the attractor of the Lorenz system (shown in green) has a larger region in the phase-space and it is chaotic. After the onset of coupling, the response system attractor shrinks (shown in blue colour), and it becomes a non-chaotic attractor.

Trajectories of the drive–response system (with the onset of coupling at $t = 20$) are shown in figures 1b–d. For this coupling scheme, variables of the drive and response systems exhibit both identical and generalized synchronization. In figure 1b, variations in x_1 and y_1 variables of both the response and drive are shown. After the onset of coupling, these are in a state of identical synchronization (IS). Since the y_2 variable of the response system is replaced with that of the drive (x_2), they are also identical to each other as shown in figure 1c. In figure 1d, trajectories of x_3 and y_3 variables of the drive and response systems are shown. Clearly, they do not overlap and are instead in a state of GS. At the onset of coupling, two response signals (of y_3 variable) are in a state of complete synchrony with each other, and develop a stable functional relationship with the corresponding trajectory of the drive (x_3 variable) as shown in figure 1d.

The field of GS was formally conceptualized by Rulkov *et al.* in the year 1995 [35]. They introduced the notion of a stable transformation function Φ

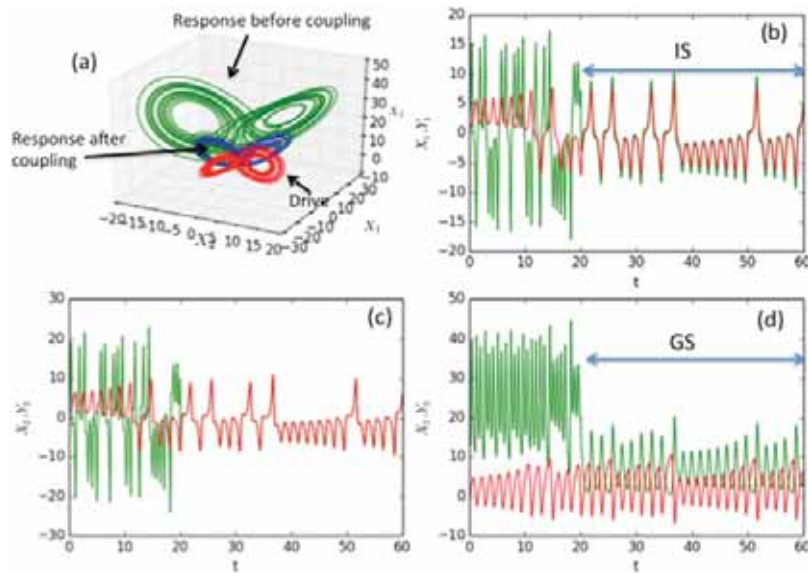


Figure 1. (a) Attractors of drive (red) and response before (green) and after coupling (blue). Trajectories of different variables before and after coupling: Drive (red) and response (green). (b) x_1, y_1 -, (c) x_2, y_2 - and (d) x_3, y_3 -variables.

which comes into existence as the response gets synchronized with the drive in a unidirectional coupling scenario, namely the systems with a skew-product structure. Mathematically, the presence of GS implies that there is a (possibly implicit) functional dependence of the response \mathbf{y} on the drive \mathbf{x} , namely

$$\mathbf{y} = \Phi[\mathbf{x}]. \quad (5)$$

They introduced the idea of mutual-false nearest neighbours to detect the onset of GS in a drive–response system, namely, the closeness in the response system implied a closeness in the drive system. Thereafter, the necessary and sufficient conditions for the occurrence of GS in unidirectionally coupled dynamical systems were discussed in terms of asymptotic stability of the response system, namely the conditional Lyapunov exponents (CLEs) of the response system become negative [36]. Techniques for approximating the form of the mapping function between two systems exhibiting GS were discussed in Ref. [37]. Here the author suggests methods to arrive at the form Φ analytically if the equations are known and numerically from the time-series data. The idea of GS in the drive–response configuration was extended to the context of autonomous spatiotemporal systems where chaotic state variables in an autonomous system can be synchronized to each other [38]. GS in the case of the unidirectionally coupled nuclear spin generator system was studied in [39].

2.1 Impact of noise in GS

More often than not, noise plays a significant role in determining the behaviour or outcome of dynamical systems. The role of noise in the systems that are

in the state of generalized synchrony has also been extensively explored. The effect of noise in numerical and experimental settings of GS has been investigated through different techniques and its role has been characterized in various studies [40–46].

In a recent study [47], the effect of multiplicative noise on GS of coupled-stochastic processes has been investigated. It was argued that, this phenomenon is the stochastic analogue of GS. This was supported by studying it in coupled flows with multiplicative noise and chemical oscillators. Measures such as correlations, permutation entropy and mutual information were employed to characterize the transition.

As a model example, Jafri *et al.* [47] considered the Brusselator system (Ref. [47]) as a drive. The corresponding chemical Langevin equations can be written as follows [48]:

$$\begin{aligned} \dot{x}_1 &= u_1(x_1, x_2) + \frac{v_1(x_1)}{\sqrt{V}}\xi_1(t) + \frac{v_2(x_1, x_2)}{\sqrt{V}}\xi_2(t), \\ \dot{x}_2 &= u_2(x_1, x_2) + \frac{v_2(x_1, x_2)}{\sqrt{V}}\xi_2(t), \end{aligned} \quad (6)$$

where ξ_i represent δ -correlated white noise, $\langle \xi_i(t) \rangle = 0$ with $\langle \xi_i(t)\xi_j(t') \rangle = \delta(t-t')\delta_{ij}$, $i, j = 1, 2$. The quantities $u_i(\mathbf{x})$ and $v_i(\mathbf{x})$, $i = 1, 2$ are defined as

$$u_1(\mathbf{x}) = c_1 - c_2x_1 + c_3x_1(x_1 - 1)x_2/2 - c_4x_1$$

$$u_2(\mathbf{x}) = c_2x_1 - c_3x_1(x_1 - 1)x_2/2$$

$$v_1(\mathbf{x}) = \sqrt{[c_1 + c_4x_1]}$$

$$v_2(\mathbf{x}) = \sqrt{[c_2 + c_3(x_1 - 1)x_2/2]x_1}.$$

As a response, one can consider a similar set of equations for the chemical reactions occurring in the Langevin–Lorenz system given by [49] (Appendix eq. (A2) of Ref. [47]),

$$\begin{aligned}\dot{y}_1 &= -\sigma y_1 + \sigma y_2 + l_1(\mathbf{y}) + \varepsilon(x_1 - y_1) \\ \dot{y}_2 &= -y_1 y_3 + r y_1 - y_2 + l_2(\mathbf{y}) \\ \dot{y}_3 &= y_1 y_2 - b y_3 + l_3(\mathbf{y})\end{aligned}\quad (7)$$

with the additional terms involving noise being [48]

$$\begin{aligned}l_1(\mathbf{y}) &= \frac{1}{\sqrt{V}} \left\{ -\sqrt{|\sigma y_1|} \eta_1 + \sqrt{|\sigma y_2|} \eta_2 \right\} \\ l_2(\mathbf{y}) &= \frac{1}{\sqrt{V}} \left\{ -\sqrt{|y_1 y_3|} \eta_3 + \sqrt{|r y_1|} \eta_4 - \sqrt{|y_2|} \eta_5 \right\} \\ l_3(\mathbf{y}) &= \frac{1}{\sqrt{V}} \left\{ \sqrt{|y_1 y_2|} \eta_6 - \sqrt{|b y_3|} \eta_7 \right\}.\end{aligned}$$

These can be derived in a straightforward manner. The diffusive coupling term in eq. (7) represents the diffusion of the species (represented by x_1) from one system to another. The noises η_i and ξ_j are independent having the following property: $\langle \eta_i(t) \rangle = 0$ with $\langle \eta_i(t) \eta_j(t') \rangle = \delta(t - t') \delta_{ij}$.

To realize the onset of GS one may define another copy of the response, namely the auxiliary unit (auxiliary system approach discussed in detail in section 3.3). Thus the same (Brusselator) drive can be coupled to a second response system which is called the auxiliary unit. When the stochastic Brusselator drive couples to the Lorenz response and the auxiliary unit, one obtains a set of coupled stochastic equations, namely eqs (6) and (7) together with

$$\begin{aligned}\dot{y}'_1 &= -\sigma y'_1 + \sigma y'_2 + l_1(\mathbf{y}') + \varepsilon(x_1 - y'_1), \\ \dot{y}'_2 &= -y'_1 y'_3 + r y'_1 - y'_2 + l_2(\mathbf{y}'), \\ \dot{y}'_3 &= y'_1 y'_2 - b y'_3 + l_3(\mathbf{y}'),\end{aligned}\quad (8)$$

where

$$\begin{aligned}l_1(\mathbf{y}') &= \frac{1}{\sqrt{V}} \left\{ -\sqrt{|\sigma y'_1|} \eta_8 + \sqrt{|\sigma y'_2|} \eta_9 \right\} \\ l_2(\mathbf{y}') &= \frac{1}{\sqrt{V}} \left\{ -\sqrt{|y'_1 y'_3|} \eta_{10} + \sqrt{|r y'_1|} \eta_{11} - \sqrt{|y'_2|} \eta_{12} \right\} \\ l_3(\mathbf{y}') &= \frac{1}{\sqrt{V}} \left\{ \sqrt{|y'_1 y'_2|} \eta_{13} - \sqrt{|b y'_3|} \eta_{14} \right\}.\end{aligned}$$

Note that here there are several noise terms, and this underscores an important distinction between the study

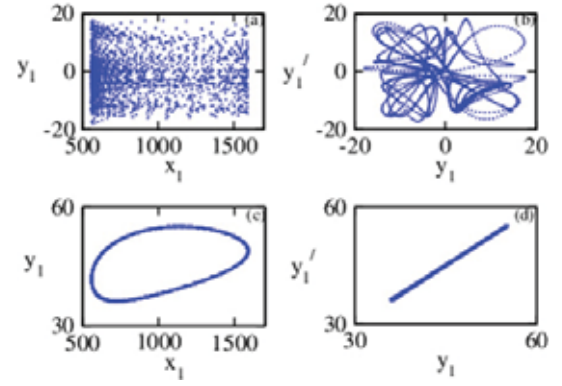


Figure 2. Phase-space plots for eqs (6), (7) and (9) as a function of the coupling. The attractor in the x_1 – y_1 plane for the drive–response system at (a) $\varepsilon = 0$, (c) $\varepsilon = 0.5$. Similar plots in the y_1 – y'_1 plane for the response and auxiliary units at (b) $\varepsilon = 0$ and (d) $\varepsilon = 0.5$.

of GS in deterministic systems as compared to that in the stochastic systems [50, 51].

Simulations for the systems with noise are carried out in the usual manner, integrating the equations of motion using a modified-Euler’s method or the fourth-order Runge–Kutta scheme. Since the coupling in this example is between two very dissimilar systems (as evidenced by the reaction schemes, eqs. (6) and (7)) therefore, it is useful to judge the extent to which the variables in the response system are uniquely determined by the drive.

Figure 2 shows the attractors which are generated by the drive–response system, projected onto the x_1 – y_1 and y_1 – y'_1 planes, where figures 2a and b show the projections for $\varepsilon = 0$, implying that there is no correlation between the drive–response and auxiliary units. If one increases the coupling, figures 2c and d for $\varepsilon = 0.5$, the two units are clearly synchronized. Since the response and the auxiliary units are in complete synchrony (see figure 2d), the systems in the drive–response configuration are in the state of weak generalized synchrony. The effect of noise was studied through phase-space analysis and it was reported that noise can either induce/enhance or destroy GS [40, 41]. At some other instance, it was also argued that the underlying mechanisms of the GS and noise induced synchrony with biased noise are similar to each other in many ways [42, 43]. The idea of GS for secure communication was discussed and its stability in the presence of noise was explored in [44–46].

2.2 Influence of delay in GS

Amongst one of the most pertinent features of dynamical systems is the presence of time delay. Delay creeps

into all natural-coupled systems due to a finite speed with which signals are transmitted from one system to another. In order to account for this, a delay τ is introduced into the coupling term and its effect has been explored in several scenarios [52–54]. The influence of delay in the realm of GS has been another area of significant research. The conditions for the existence of the GS between two linearly and nonlinearly coupled chaotic non-identical models with variable feedback delay were discussed in [55]. Extension of this approach to other chaotic systems was also described.

A novel coupling scheme with different coupling delays was presented to achieve GS [56]. In this case it was theoretically shown that it is possible for the network to switch between different synchronization regimes and the results were verified by numerical simulations. In a separate study, detection of GS in modulated-time delayed systems was proposed by a method based on Krasovskii–Lyapunov theory [57, 58]. The nature of transition to GS in a system of two-coupled scalar piecewise linear time-delay systems was studied using an auxiliary system approach and it was shown that transition to GS occurs via an on–off intermittency [59].

2.3 Effect of multistability on GS

Dynamical systems with symmetry may lead to multistability. In multistable systems, trajectories evolve to different attractors depending on the basins of attraction of different initial conditions. The concept of the existence of unique functional relationship between the drive and response can break down when the response system has multiple basins of attraction [60]. These issues, where the response exhibits multistability, were studied in [61]. The reason for multistability was explored and was characterized in terms of uncertainty exponents.

2.4 Relay and remote synchronization: Manifestation of GS

Relay and remote synchronization, despite having been introduced in different contexts, strongly reveal the characteristics of GS. Both forms of synchronizations share a common mechanism, where two systems that are not connected directly synchronize via an interaction with a common hub node. The groups of nodes in synchronization under the action of a hub node relay the information. In both situations, a functional relationship develops between the group of nodes and hub, and therefore the regime of GS develops in the system.

Remote synchronization was first reported in a star network [62], where all peripheral oscillators are in synchronization but dynamics of hub oscillator is

de-tuned from the rest. Later, this phenomenon was also reported in complex networks of symmetrical nodes, where groups of nodes at distant locations (without direct connection with each other) in the network display patterns of synchronization with the same phase. The other groups have the same frequency, but different phase lags [63, 64]. Thus, emergence of GS in complex networks has also become an area of active research in recent years (discussed in section 5).

Examples of relay synchronization are found in systems of three oscillators which are coupled bidirectionally along a chain with time-delay [65–67]. The presence of coupling delay induces stability in the system resulting in the onset of relay synchronization. In the regime of relay synchronization, outer peripheral oscillators achieved CS through indirect coupling with the middle relay unit, whose dynamics either lags or leads the synchronous state [66, 67]. Both relay and remote synchronization can be viewed as a manifestation of GS. GS in relay systems with instantaneous coupling was proposed by Gutiérrez *et al.* [68]. Gutiérrez *et al.* studied dynamics of relay systems, and they demonstrated the existence of GS in relay by providing numerical and experimental evidences.

3. Detection of generalized synchrony

Over the years, several methods have been proposed for the detection of GS, including mutual-false nearest neighbour [35], replica method or auxiliary system approach [25], synchronization likelihood approach [69] and statistical methods like Bayesian inference [70] amongst others.

Pyragas discussed various tools for detecting and analysing the properties of GS [71]. Symbolic dynamics was employed to study GS, and a change in conditional entropy is used as a marker to detect the onset of GS [72]. For experimental data, ‘synchronization likelihood’ was proposed to detect GS for multivariate data sets [69] which may be non-stationary such as electroencephalogram (EEG), magnetoencephalogram (MEG) [73] etc. We discuss some of these works briefly.

3.1 Mutual-false nearest neighbour

This was the first numerical method which was proposed to detect GS [35]. This method allows us to detect the presence of continuous functional relationship between the drive and response, and it is based on reconstruction of delay phase-space. If a synchronizing relationship of the form $\mathbf{y} = \Phi[\mathbf{x}]$ (eq. (5)) occurs, it means that the motion in full phase-space of the drive and response has collapsed onto a subspace which is

the manifold of synchronized motions. By observing the evolution of the response system in one scalar variable $r(t)$, we can reconstruct the chaotic trajectory $r(t)$ in the embedding phase space R_E from the value of the trajectory at time t and at several values of delay τ using d_r dimensional vectors

$$r(t) = (r(t), r(t + \tau), r(t + 2\tau), \dots, r(t + (d_r - 1)\tau)). \quad (9)$$

If synchronization occurs, we can expect a continuous functional relation

$$r(t) = \psi(d_r), \quad (10)$$

where $d_r(t)$ is the chaotic trajectory reconstructed in the embedded space D_E from scalar variables taken from the drive system. To detect the existence of ψ , the idea of mutual-false nearest neighbour is explored, which tests whether neighbourliness in D_E translates in a practical, numerical sense to neighbourliness in R_E .

3.2 Lyapunov spectra

Two chaotic systems driven by a common signal can result in synchronization of the two systems. This occurs when the signs of the Lyapunov exponents (LEs) of the subsystems are all negative [16]. Another study that investigated the synchronization stability of two-coupled units introduced an idea of complete replacement [74]. In this technique, the signal from one unit is transferred to the other. Thus, the response is treated as a separate dynamical unit driven by the common variable and the LEs for the response subsystem alone are called as conditional LEs. It was argued that the criterion for the smoothness of ϕ in any drive response scenario is that the least negative conditional LE of the response must be less than the most negative LE of the drive.

Further, if the drive–response system defined by eq. (1) is expressed explicitly in terms of coupling, then we have

$$\begin{aligned} \dot{\mathbf{x}} &= F(\mathbf{x}), \\ \dot{\mathbf{y}} &= F(\mathbf{y}) + \alpha \mathbf{E}(\mathbf{x} - \mathbf{y}), \end{aligned} \quad (11)$$

where \mathbf{E} is the coupling matrix and α is the coupling strength. One can study the system in terms of the transformed variables that correspond to the synchronization manifold and the transverse manifold. To see this, let us consider the drive and response to be three dimensional such that the variables are given by $\mathbf{x}^T = [x_1, x_2, x_3]$ and $\mathbf{y}^T = [y_1, y_2, y_3]$. The variables of the synchronization manifold are defined as $x_{||} = x_1 + y_1$, $y_{||} = x_2 + y_2$ and $z_{||} = x_3 + y_3$ whereas the variables of the transverse manifold are given by $x_{\perp} = x_1 - y_1$, $y_{\perp} = x_2 - y_2$ and $z_{\perp} = x_3 - y_3$. Clearly, we need to have x_{\perp}, y_{\perp} and z_{\perp}

go to zero as $t \rightarrow \infty$. This leads to requiring that \dot{x}_{\perp} , \dot{y}_{\perp} and \dot{z}_{\perp} be stable at $(0, 0, 0)$. In the limit of small perturbations, one can find the variational equation for the response given by,

$$\begin{pmatrix} \dot{x}_{\perp} \\ \dot{y}_{\perp} \\ \dot{z}_{\perp} \end{pmatrix} = F(\mathbf{x}) - F(\mathbf{y}) = DF \cdot \begin{pmatrix} x_{\perp} \\ y_{\perp} \\ z_{\perp} \end{pmatrix}, \quad (12)$$

where DF represents the Jacobian of the response. The equation clearly represents the dynamics of the perturbations transverse to the synchronization manifold. One can use this to evaluate the transverse LE. If the largest transverse LE is negative, the perturbations damp out and consequently the synchronized dynamics is stable. Thus, one can say that in order to achieve GS the transverse LEs must be negative.

In another study of GS using conditional LEs [75], it was argued that the GS of the unidirectionally coupled systems can be detected by predicting the state of the response system using a time series from the drive system. While considering the GS of identical systems, a pair of unidirectionally coupled identical Chua oscillators were considered. The CLE was calculated by computing the Jacobian matrix of the vector field in terms of the state vectors of the drive system. Since CLE was calculated to study the synchronization of identical systems, it was called as IS-CLE. However, for investigating the mutual synchronization of a pair of non-identical response systems, the Jacobian was determined using the response state, and hence the resulting CLEs were termed as GS-CLE. It was shown that the IS occurs if both the sets coincide while for GS they are different. This was further verified by calculating other order parameters.

Extensive work in the case of exploring the possibility of GS in the popular Ginzburg–Landau equations was performed by the authors in Refs [76–78]. In [23], a pair of unidirectionally coupled non-identical Ginzburg–Landau equations were considered; the transition to phase synchronization was studied by calculating phases. If the coupling parameter was further tuned, the functional relationship between the variables of the drive and response was observed which was further justified by calculating all transversal LEs. There are other instances where GS was explored in the unidirectionally coupled Ginzburg–Landau equations by using the kernel method [76–78].

The presence of parameter mismatch in the coupled units can affect the state of CS [55]. It was demonstrated that in the presence of parameter mismatch, the mode of synchrony changes from being identical to generalized synchrony by using the Krasovskii–Lyapunov functional approach.

3.3 Auxiliary-system approach

Another important work directed towards detecting the appearance of GS in skew-structured coupled dynamical systems was reported by Abarbanel *et al.* [25]. The auxiliary system approach has become a standard method to detect the presence of GS in many theoretical and experimental works. In this technique, a replica of the response system is taken, and the dynamics between the response and its replica is monitored. A complete synchrony (which is easier to detect) between the response and its copy driven by the common autonomous drive system signals the onset of GS (illustrated in figure 3). It is widely used in various unidirectionally coupled chaotic oscillators, mutually coupled systems and in networks of chaotic dynamical systems.

Breakdown of the auxiliary system approach was also reported in bidirectionally coupled systems [60, 79]. The inability of the auxiliary-system approach to correctly detect the GS regime was demonstrated in two bidirectionally coupled Rossler and Lorenz systems [60]. Kata *et al* considered a system of Mackey–Glass oscillators in a unidirectional ring [80]. In their work, measures to quantify generalized and phase synchronization from noise-free time series of two oscillators are studied using the auxiliary systems approach, and it was found that the latter was inconsistent to detect synchronization in a generalized way.

An idea of intermittent GS was introduced, where the appearance of GS is preceded by intermittent behaviour [81]. It was observed that there are time intervals during which the synchronized oscillators are interrupted by non-synchronous bursts. Here states of the response and auxiliary systems $|y - y'|$ show that the laminar phase corresponds to the regime of GS and the turbulent phase to desynchronized states.

To illustrate some of these ideas, we show an example of two-coupled identical one-dimensional maps considered by Pyragas [82]

$$\begin{aligned} x(i+1) &= f(x(i)) \\ y(i+1) &= f(y(i)) + k\{f(x(i)) - f(y(i))\} \end{aligned} \quad (13)$$

with the auxiliary system given by

$$y'(i+1) = f(y'(i)) + k\{f(x(i)) - f(y'(i))\}. \quad (14)$$

At any given value of k (coupling strength), eq. (13) admits CS. Figure 3 shows the phase portraits of the system for logistic maps given by $f(x) = ax(1 - x)$ at $a = 4$ for various values of the coupling constants k in the x - y and y - y' planes. At low values of k , there is no synchronization between the response and the drive as

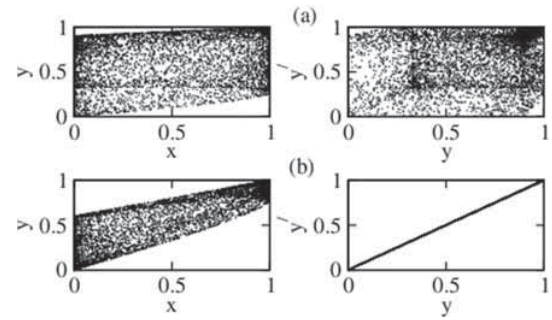


Figure 3. Phase portraits in the x - y and y - y' planes of the coupled logistic maps for various values of the coupling strength k : (a) $k = 0.1$, the unsynchronized state and (b) $k = 0.4$, the onset of GS.

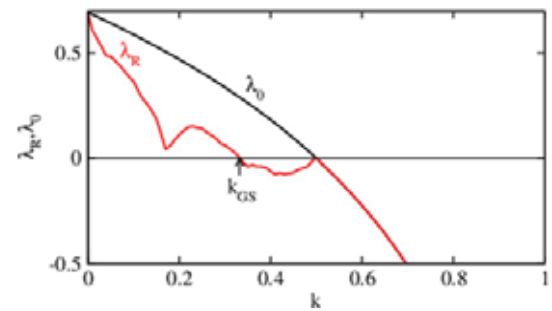


Figure 4. Variation of the CLEs (λ_R) and transverse-LEs (λ_0) with the coupling strength k indicating the onset GS.

shown in figure 3a. On increasing k , synchrony first sets in between the response and the auxiliary unit as shown in the right panel of figure 3b. The drive and response units synchronize at higher values of k (not shown here). The threshold value for the occurrence/onset of GS can be calculated using the CLE given by

$$\lambda_R = \ln(1 - k) + \lim_{n \rightarrow \infty} \frac{1}{n} \sum_{i=1}^n \ln |f'(y(i))| \quad (15)$$

that defines the stability of the invariant manifold $y' = y$. The transverse LE of the invariant manifold $y = x$ is given by

$$\lambda_0 = \ln(1 - k) + \lim_{n \rightarrow \infty} \frac{1}{n} \sum_{i=1}^n \ln |f'(x(i))|. \quad (16)$$

As shown in figure 4, the onset of GS is obtained for k_{GS} where the CLE becomes negative.

3.4 Statistical methods

Statistical frameworks can overcome the weakness of the auxiliary system approach to detect GS [70, 83]. It is often desirable to detect synchronization from measured time series. However, there are difficulties

associated with inference from time-series data because of unknown parameters in these models, and other conditions imposed on the system.

A statistical modelling framework for the detection of nonlinear interactions between two time series was proposed by Schumacher *et al.* [70]. A time series $y(t)$ was estimated from another signal $x(t)$ by using a Volterra series operator F on $x(t)$, where F is called the functional synchrony model (FSM). The method was efficient in several-coupled chaotic systems for which generalized nonlinear synchronization is known to exist. Framework of nonlinear synchronization as a formalization of complex interactions is an important aspect to understand information processing in the brain, wherein, the dynamics between various regions is coordinated and synchronized. Stankovski *et al.* proposed Bayesian inference-based method that can test whether or not the system is in the GS regime by evaluating the asymptotic stability of the inferred driven oscillator [83]. Their method can distinguish whether two oscillators are simply coherent without functional dependence, or synchronized due to interactions, thus advancing characterizing tools for the detection of GS from time-series data. Another important work particularly in the analysis of time-series data is reported in Ref. [84]. A unified framework was also put forward to study GS by making use of the kernel method resulting in a canonical correlation coefficient of kernel that was argued to be a suitable order parameter for detecting GS [85].

4. Scenarios of GS: Strong and weak GS

The nature of the mapping function Φ was investigated in a few works [82, 86–88]. It turned out that this function need not be differentiable even if the vector fields F (drive) and G (response) are continuous and smooth. In general, Φ can be smooth or non-smooth, thus distinguishing the regimes of strong and weak GS, respectively, namely a differentiable Φ suggests that the GS is strong (SGS), and, contrastingly, if it is not differentiable, it is termed weak GS (WGS). Also, if Φ is the identity function, we get CS as a particular case of GS.

In a typical situation, with a variation in the coupling strength the differentiability properties of the function Φ undergo a change leading to a transition between SGS and WGS [89]. Several works [90–92] have shown that in chaotically driven nonlinear systems, WGS can arise through distinct dynamical routes in a manner similar to the creation of strange non-chaotic attractors in a quasiperiodically driven system [93]. These works have established a unifying framework of the bifurcation routes in a class of

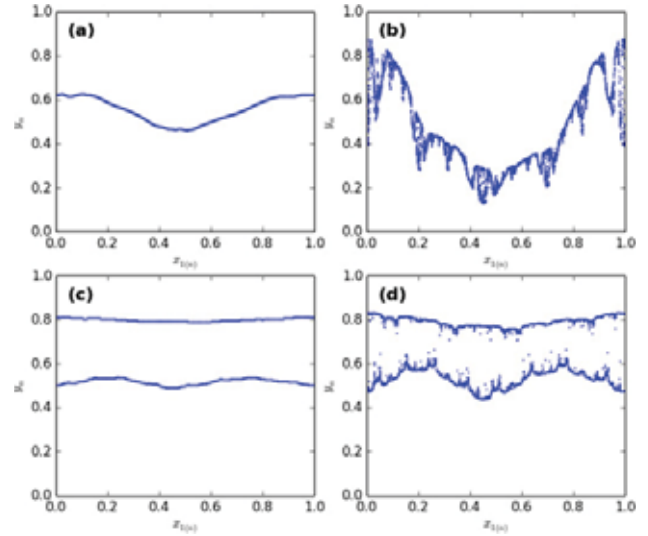


Figure 5. SGS and WGS in the logistic map (eq. (17)) driven by chaotic Baker’s map (eq. (18)). (a) and (b) Transition from SGS to WGS through fractalization. (c) and (d) Transition from SGS to WGS through a doubling collision route.

aperiodically forced nonlinear dynamical systems. In a separate study, Keller *et al.* considered a chaotically driven monotone map and studied the geometry of the limit set formed in the regime of WGS [94]. The fractal dimension of the set of zeros has been studied both numerically and analytically. The stability index and the dimension spectrum were analysed. In the regime of WGS, stable aperiodic dynamics are realizable. This has been a major objective in the study of driven dynamical systems both from the point of view of applications in secure communication and to understand sustenance of rhythms in interacting dynamical systems [95].

SGS and WGS in a chaotically driven logistic map are shown in figure 5. The governing dynamical equation for the response system is given by

$$y_{n+1} = \alpha y_n (1 - y_n) (1 + \varepsilon \cos 2\pi x_{1n}), \quad (17)$$

where α and ε are system parameters. The chaotic drive is provided by the x_1 variable in the generalized Baker’s map,

$$x_{1(n+1)} = \begin{cases} bx_{1n}, & x_{2n} < a, \\ b + (1 - b)x_{1n}, & x_{2n} \geq a, \end{cases} \quad (18a)$$

$$x_{2(n+1)} = \begin{cases} x_{2n}/a, & x_{2n} < a, \\ (x_{2n} - a)/(1 - a), & x_{2n} \geq a \end{cases} \quad (18b)$$

with $a = b = 0.45$.

Figures 5a and b show the transition of SGS to WGS through fractalization and graph-doubling collision routes. For $\alpha = 2.3$ and $\varepsilon = 0.2$ in eq. (17), we have SGS as shown in figure 5a. Here the graph between the variables of the drive and response is smooth. On the other hand, on increasing the coupling strength to $\varepsilon = 0.7$, we have WGS in figure 5b where the graph is non-smooth. A scenario of the doubling-collision route, where collision of the doubled graph with its unstable parent results in the transition of SGS to WGS, is shown in figures 5c and d. For $\alpha = 3.2$ and $\varepsilon = 0.05$, we have SGS with a smooth-doubled graph in figure 5c. WGS with a non-smooth graph in figure 5d is obtained for $\alpha = 3.2$ and $\varepsilon = 0.15$. Such transitions are also observed in continuous-time dynamical systems as well [91, 92].

Pyragas [82] and Hunt, Ott and Yorke [86] amongst several others, have addressed the issue of detecting SGS to WGS transition by suggesting several markers or numerical/analytical tools which undergo a change as the function Φ changes the nature of its differentiability. Tools such as mean thickness, cross-correlation, Lyapunov dimension [96, 97] and CLEs [16] amongst others are used extensively in the literature to this end. SGS occurs if the response system has no effect on the global Lyapunov dimension estimated using the Kaplan–Yorke conjecture [96]. Another method to estimate the CLE from the time series of the drive and response was proposed in Ref. [98]. The technique was illustrated for the coupled maps and coupled-chaotic flows. This approach was also based on the comparison of the global Lyapunov dimension with the dimension of the drive. We can estimate the smoothness of the synchronization manifold using this method.

In another attempt to explore these issues, Hunt *et al.* [86] proposed conditions under which the response of the system to a chaotic drive is a smooth function of the drive state namely the differentiable generalized synchronization (DGS). This simply means that there exists a functional relationship Φ between the variables of the drive and response and that Φ is continuously differentiable. If DGS does not hold, the degree of non-differentiability was quantified using the Hölder exponent $\gamma(\mathbf{x})$ which is defined for any point (\mathbf{x}, \mathbf{y}) . Here, \mathbf{x} is on the drive attractor and $\mathbf{y} = \Phi(\mathbf{x})$. For points \mathbf{x} and $\mathbf{x} + \delta$ on the drive attractor,

$$\gamma(\mathbf{x}) = \liminf_{\delta \rightarrow 0} \frac{(\log \|\Phi(\mathbf{x} + \delta) - \Phi(\mathbf{x})\|)}{\log(\|\delta\|)}. \quad (19)$$

$\gamma(\mathbf{x}) > 0$ if $\Phi(\mathbf{x})$ is continuous at \mathbf{x} while for $\gamma(\mathbf{x}) < 1$ Φ is not differentiable. $\gamma(\mathbf{x}) = 1$ implies that $\Phi(\mathbf{x})$ is differentiable at \mathbf{x} .

Several other methods appear in the literature wherein the authors propose different techniques for

the detection of the non-differentiability of the implicit function [88, 99]. Some rigorous results on the continuity of the implicit function have been obtained by Afraimovich *et al.* in Ref. [100], but applicability of these results in the general case is difficult. A practical method for detecting this transition has been proposed by Manchanda and Ramaswamy in Ref. [101]. Here the authors show both analytically as well as numerically that instantaneous mode frequencies (IMF) and their corresponding variances present in the signals coming from a drive–response system can be used as suitable order parameters to distinguish between regimes of SGS and WGS. To demonstrate this technique, the authors study a chaotically modulated forced Duffing oscillator [91] which is given by the equations,

$$\begin{aligned} \dot{y}_1 &= y_2 \\ \dot{y}_2 &= -hy_2 - y_1^3 + [1 + A(\cos y_3 + a_r x_1)]y_1 \\ \dot{y}_3 &= 1. \end{aligned} \quad (20)$$

The total modulation in eq. (20) is a superposition of two signals: a sinusoidal drive, and $x_1(t)$ which we take here to be the output of the Rössler drive specified as

$$\begin{aligned} \dot{x}_1 &= \alpha(x_2 + x_3) \\ \dot{x}_2 &= \alpha(x_1 + ax_2) \\ \dot{x}_3 &= \alpha[b + x_3(x_1 - c)] \end{aligned} \quad (21)$$

with $a = b = 0.2$, $\alpha = 1.49$. The coupling between the drive and response is fixed with a_r at 0.125, $h = 0.2$, $A = 0.15$, and the Rössler oscillator parameter c is used as a control.

In figure 6, we show the variation of the frequency (ω) as well as its variance (σ) for the largest mode in (a), (b) and for the second largest mode in (c), (d) as a function of the parameter c in eq. (21). These figures clearly show a sharp change in the critical value of the parameter c , $c \approx 5.18505$ which is in agreement with the transition value reported in Ref. [91] calculated using other measures.

GS has been characterized into three distinctive types based on the roles played by the drive and response units [102]. The study of Hölder continuity of GS was performed based on the modified-system approach, thereby classifying GS into three types namely, equilibrium GS, periodic GS and C-GS [87, 103, 104].

5. GS in complex systems

Complex topologies exist in many artificial and natural networks [105]. It is composed of many parts,

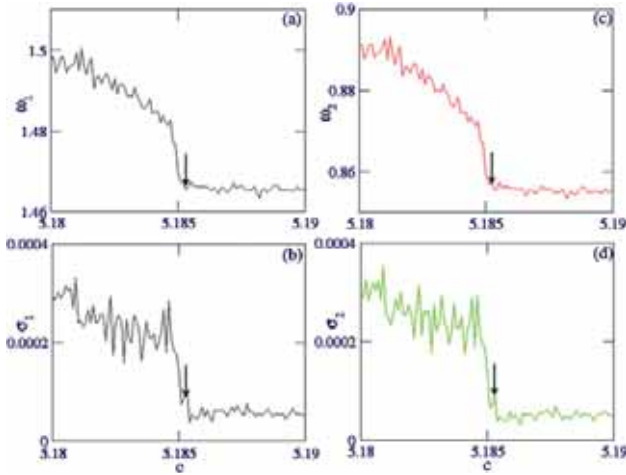


Figure 6. Transition from WGS to SGS in the Rössler drive–Duffing response system. (a), (b) The largest frequency IMF ω_1 and its variance σ_1 and (c), (d) second largest frequency IMF ω_2 and its variance σ_2 as a function of the parameter c (cf. eq. (21)). The transition from WGS to SGS, which is located at the point when the variance as well as the frequency show a sudden decrease, occurs at $c \approx 5.18505$. Here the response variable $y_2(t)$ is used for the analysis.

which are interrelated with each other in a complicated way, possessing both ordered and disordered dynamics. Most biological and physical systems have the characteristics of complex networks since they consist of multiple non-identical interacting constituent units. Spatiotemporal dynamics (both ordered and disordered) generally appear in complex systems regardless of whether the constituent units are identical or non-identical, and also even in the presence of other heterogeneities [106–108]. Prevalence of networks is ubiquitous in nature and the presence of GS has been established in systems that span across various disciplines. Thus, it becomes interesting to see how the phenomenon predominantly observed in a two-system configuration translates in the scenario of several interacting units put together.

A technical issue is the question of mathematical formalism. Mathematical tools to study GS on complex networks have been unclear over the years due to its complexity. However, in the recent past, researchers have begun to study synchronization of networks and extended the formalism of GS from a simple drive–response system consisting of two dynamical systems to complex networks consisting of several non-identical constituent units [68, 83, 109].

5.1 GS in complex networks

The framework of GS has been successful in tracing the evolution of different-coupled systems in complex

networks [110–113]. Typical networks include modular networks [68, 79], random networks [110], scale-free networks [109] and small-world networks [114]. Techniques developed to detect the GS in the drive–response system are able to establish the presence of functional relationship between states of groups of nodes and other groups [113]. Consider the following linearly coupled identical oscillators on a network:

$$\dot{x}_i = \mathbf{F}_i(x_i) - \varepsilon \sum_j a_{ij} H(x_i - x_j), \quad (22)$$

where $i = 1, \dots, N$, x_i denotes the dynamical variables of node i , $\mathbf{F}_i(x_i)$ is the local vector field governing the evolution of x_i in the absence of interactions with other nodes, a_{ij} is the element of the network adjacency matrix A , H is the output matrix and ε is the coupling strength. For any given node in a network, the coupling from other nodes can be regarded as a kind of drive. Thus, one can apply the auxiliary-system approach in networks wherein a replica of each oscillator in the original network (response) is used to monitor the synchronized motions between the response given by eq. (22) and the auxiliary system that can be expressed as

$$\dot{x}'_i = \mathbf{F}_i(x'_i) - \varepsilon \sum_j a_{ij} H(x'_i - x_j). \quad (23)$$

This method can be implemented both numerically and experimentally. Numerically, we can examine the following local distance of GS between a node and its auxiliary counterpart:

$$d(\varepsilon, i) = \frac{1}{t_2 - t_1} \sum_{t_1}^{t_2} |x'_i - x_j|, \quad (24)$$

where t_1 is chosen to be larger than the typical transient time of the local dynamics $F_i(x_i)$. Operation of GS between the driver nodes and response nodes in the network is confirmed when there is a complete synchrony between the response and the auxiliary system $x_i = x'_i$, which in this case is given by $d(\varepsilon, i) \rightarrow 0$. But, the auxiliary system approach is only one sufficient condition.

GS in networks via adaptive couplings was also studied in [115]. Shang *et al.* [110] chose suitable driving signals and constructed the response network with a predefined functional relationship such that the drive and response networks are generally synchronized. Huang *et al.* [109] considered synchronization in scale-free networks consisting of bidirectionally coupled chaotic oscillators. They apply the auxiliary-system approach to examine GS in a scale-free network of identical oscillators, and found that GS started

from the hubs of the network and gradually spread throughout the whole network as the strength of coupling is changed. The onset of GS in a network of identical oscillators is a consequence of heterogeneity of the degree of scale-free networks. Such results provide an insight into the spread of the synchronization process, and a perspective to understand the role of topological hubs in imparting global dynamics in complex networks. GS is now a well-established framework for analysing spatiotemporal coherence in complex networks [109, 113, 116].

5.2 GS and chimera states

In recent years, several studies have started investigating the interplay of chimera states [117, 118] across separate networks [119–121] within the framework of GS [119]. Chimera states are spatiotemporal segregation consisting of stable coherent and incoherent groups, which coexist. There are growing experimental and numerical evidence [122] with strong theoretical frameworks [117, 123] that they manifest themselves in many natural and artificial networks. Earlier, most of the works in the study of chimera states have been focused on isolated networks. Recently, Andrzejak *et al.* have shown that chimera states across different interacting networks can result in a state of GS [119]. The findings established the fact that a network can maintain its spatiotemporal segregation of synchronized and desynchronized clusters, and at the same time maintain synchronization as a whole with another network.

An analysis of chimera states as drive–response systems was performed by Botha and Kolahchi [121]. Their work is an attempt to bridge the gap between GS and chimera states. They have shown that spatiotemporal segregation of stable coexisting coherent and incoherent groups can be studied in terms of Pecora and Carroll's drive–response theory [74]. The incoherent group acts as a drive to synchronize the coherent group, and the coherent group plays the role of a response. The CLEs were evaluated and they were found to have the characteristic distribution that was reported previously for chimera states [124]. The onset of chimera states was studied within the framework of the drive–response system of GS in Ref. [120].

6. Experimental observations and applications

One of the earlier experimental observation of the occurrence of GS was made on the microwave oscillator [125]. This study was performed both numerically and experimentally where GS was detected by analysing the power spectra of the chaotic oscillators. Since the dynamics of the response changes sufficiently at the onset of GS it is expected that these transformations are also

manifested in the power spectra of the response. These qualitative changes in the power spectra have been detected by means of an order parameter. Other instances of experimental evidence can be found in [126]. GS was also studied in two resistive–capacitive–inductive-shunted Josephson junctions [127].

Tang *et al.* [128] showed that the chaotic dynamics of a single-mode laser under the influence of nonlinear resonant interaction can become functionally related to the chaotic driving signal. On increasing the coupling strength further, the dynamics of the driven system approaches the dynamics of the drive [29]. In a separate study [27], one-way coupled electronic circuits displaying GS were considered. Occurrence of WGS and SGS that corresponds to the existence of a non-smooth and smooth functional dependence between the variables of the drive and response was reported. In [30], two spatially extended chemical systems were considered and it was observed that by making use of continuous feedback, it was possible to achieve GS. Chaotic communication of a signal using the technique of GS was proposed in [31, 32]. It was argued that using GS in communication is more advantageous because of its more effective secrecy which is there because of the unknown functional form. In [33], it was shown that GS can be used to break chaotic switching schemes.

In a recent work by Chishti and Ramaswamy [129], a general procedure was outlined to guide the joint dynamics of two-coupled systems onto a specific transversally stable invariant submanifold. The target was to achieve a specific state of GS where synchronization is stable under transverse perturbations. Thus, a design strategy was chosen such that the trajectories in the system are attracted to the submanifold and the coupling provides these forces of constraint. These results have been presented to complement synchronization engineering wherein the functional form of the coupling term can be used as an instrument of control [130] to achieve the required state of synchronization.

In another application of the phenomenon of GS, it was proposed that one can construct public key cryptosystems by making use of coupled-map lattices under generalized synchrony [131]. The techniques to break the secure communication methods based on projective synchronization [132] were proposed in Ref. [133]. GS was experimentally studied by setting a state-feedback scheme resulting in illustrations that were used to corroborate the theoretically observed results [134].

7. Future outlook: Topological transitions in GS

Topological methods can be employed to analyse the time series of the response units. A change in the

topological structure that occurs in the response can be studied and validated by comparing it with the techniques from the metric approach. Topological methods deal only with the time series, thereby rendering this approach as an appropriate means to detect GS experimentally. We build upon this idea and present here some preliminary results from an ongoing work [135]. Here we leverage our understanding of the structure of the unstable periodic orbits (UPOs) that are present in the skeleton of a chaotic attractor, to investigate the behaviour of a dynamical system, thereby adopting a topological approach to understand GS. The effect of these UPOs on the existence or sustenance of GS in a drive–response scenario was discussed in [136, 137]. Another such factor that plays a major role in the loss of GS is the so called subharmonic transition [138].

Creation of a strange attractor is based on two mechanisms, namely: stretching and squeezing that are responsible for ‘sensitive dependence on initial conditions’ and ‘recurrence’. Mindlin and Gilmore [139] put forward a procedure to perform topological analysis wherein periodic orbits are extracted from the time series by the method of close returns. These periodic orbits are then embedded in a three-dimensional phase-space. The linking number and relative rotation rates of these periodic orbits can be determined which can be used to identify the underlying template or knot holder. This template can provide the model for the dynamics that generates the chaotic time-series data.

Using techniques described in [139], our endeavour will be to unravel the changes in the topology of the response as a result of GS. As a model example, we consider a nonlinear electric circuit as a drive whose dynamical equations are given by

$$\begin{aligned}\dot{x}_1 &= x_2 \\ \dot{x}_2 &= x_3 \\ \dot{x}_3 &= \mu x_1(1 - x_1) - x_2 - \gamma x_3\end{aligned}\quad (25)$$

with $\mu = 1$ and $\gamma = 0.5$. The response is the Rössler oscillator given in eq. (21), with $a = b = 0.2$ and $c = 5.7$. Here the response system is coupled to the drive through the y_2 variable, namely

$$\dot{y}_2 = \alpha(y_1 + ay_2) - \varepsilon'(y_2 - x_2),\quad (26)$$

and an auxiliary unit identical to the response given by

$$\begin{aligned}\dot{y}'_1 &= \alpha(y'_2 + y'_3) \\ \dot{y}'_2 &= \alpha(y'_1 + ay'_2) + \varepsilon'(x_2 - y'_2) \\ \dot{y}'_3 &= \alpha[b + y'_3(y'_1 - c)].\end{aligned}\quad (27)$$

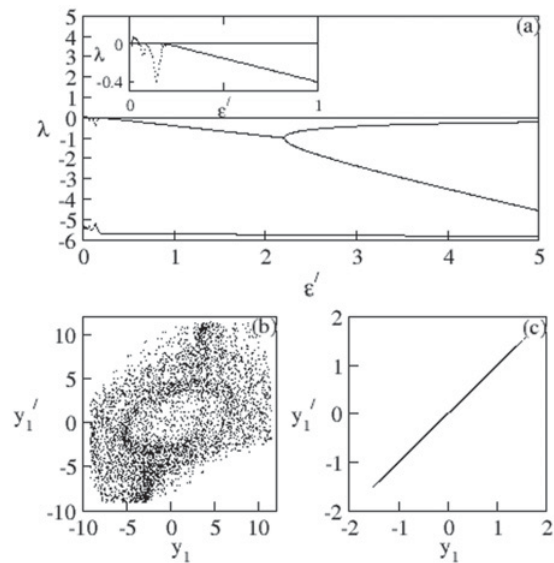


Figure 7. (a) Variation of the CLEs for the drive–response system given by eqs. (25) and (21) with the coupling. In the inset we show a small region where GS occurs. The plot between the variables of the response y_1 (cf. eq. 21)) and the auxiliary unit y'_1 (c.f. eq. 27)) (b) before GS, i.e. at $\varepsilon' = 0$ and (c) after GS at $\varepsilon' = 0.3$.

We study the change in the dynamics of the coupled system by calculating their CLE. In figure 7a, the CLEs are plotted with the coupling ε' . The largest CLE is plotted with the solid line whereas the second and the third largest are plotted using dotted and dashed lines, respectively. In a drive–response configuration, the onset of GS is usually characterized by the largest CLE which becomes negative. This can also be verified by considering an auxiliary system approach, where the response and the auxiliary units are in complete synchrony when the drive and response are in GS. As shown in figure 7b, at $\varepsilon' = 0$ the response (y_1) and the auxiliary unit (y'_1) are not in complete synchrony whereas in figure 7c, at $\varepsilon' = 0.3$ ($\alpha = 1$), they are in complete synchrony [140].

Typical attractors for the response before and after GS are shown in figures 8a and b respectively, which reflect that there is a significant change in the topology as GS sets in. In order to discern this change, one has to probe deeper into the orbits of the attractor, for which we resort to the idea of extracting periodic orbits by the method of close returns. Thus, in any time series ($x(i), i = 1 \dots N$), close return segments can be recognized by making a two-dimensional close returns plot of $|x(i) - x(i + p)| < \delta$. The pixel (i, p), which is coloured black, corresponds to the case where $|x(i) - x(i + p)|$ is below some threshold value δ given by $\delta \sim 10^{-2} \times \{\text{Max}[x(i)] - \text{Min}[x(i)]\}$. The plots for close returns are shown in figures 8c and d for the response

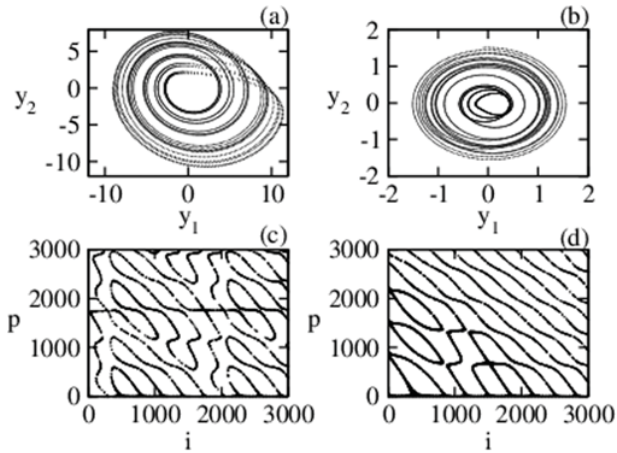


Figure 8. Dynamics of the response (eq. (21)) before and after the onset of GS. The attractor of the response system at (a) $\varepsilon' = 0$ and (b) $\varepsilon' = 0.3$. The close return plot for the response at (c) $\varepsilon' = 0$ and (d) $\varepsilon' = 0.3$.

at $\varepsilon' = 0$ and $\varepsilon' = 0.3$, respectively [135]. We can also plot a close return histogram for large data set which can be calculated as

$$H(p) = \sum_i \Theta(\delta - |x(i) - x(i + p)|), \quad (28)$$

where Θ is the Heavyside function. One can expect that the chaotic time series gives a series of peaks. As shown in figures 9a and b we have histograms for the close return for the drive and response at $\varepsilon' = 0$ and at $\varepsilon' = 0.3$ respectively. It is clear that the histograms of the drive and response before GS differ qualitatively from each other. This is expected because we have chosen completely different dynamical units. Nevertheless, as one enters the regime of GS, we observe that the histograms of the close return for the two units are very close to each other. These results suggest that the onset of GS is accompanied by the topological closeness in the attractors of the drive and response. It is therefore important that we extract the periodic orbits and embed them into three-dimensional phase space. Further, one can calculate the linking number and relative rotation rate which in return will help us to quantify the topological changes that take place at the onset of GS.

8. Summary and discussion

In the present report, we have reviewed the idea of GS, the most fundamental temporal correlation which occurs between unidirectionally coupled systems, wherein, the variables of the response can be

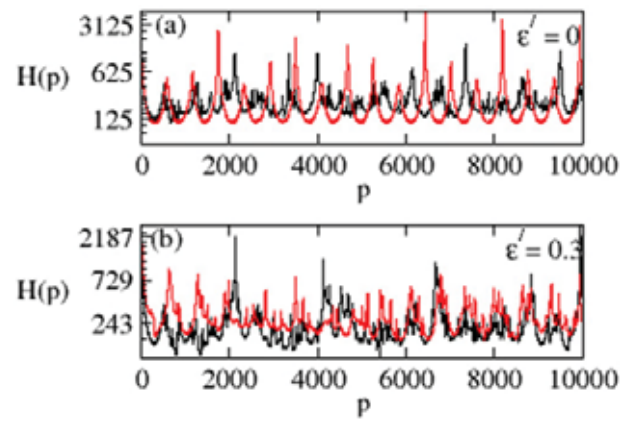


Figure 9. Histogram for the close return for the response (red or grey) is shown in (a) for $\varepsilon' = 0$ and (b) $\varepsilon' = 0.3$. The black curve in each plot that corresponds to the histogram for the close return of the drive is for comparison with that of the response.

expressed as a function of the variables of the drive. This function may or may not be smooth, thus GS is categorized into WGS (non-smooth Φ) and SGS otherwise. Several markers capable of detecting the change in the differentiability of Φ and their relative merits are also discussed in this work. Since natural systems are influenced by noise, several studies were devoted to unravel this phenomenon in the presence of noise which is found to play an important role in the onset of GS in particular and in sustenance or breakdown of synchrony in general. Another pertinent feature found in interacting dynamical systems is the finite speed with which signals travel from one system to the other resulting in the delay in transmission. Various scenarios of GS with time delay have been reported in this work.

Several techniques that have been used to detect GS are summarized in this report. The idea of mutual-false nearest neighbour based on the embedding techniques, the Lyapunov spectra and the auxiliary system approach discussed here are amongst the popular ones. Statistical methods, namely Bayesian inference and FSM, which were used to study GS are also described here. In addition to this, various experimental studies in several domains such as lasers, electronic circuits, communication etc.. establish that GS pervades most physical systems.

Though GS was originally introduced in the context of only two-coupled units, namely the drive and response, but this idea was later extended to the study of multiple-coupled units. These units may interact with each other through different configurations leading to the idea of relay and remote synchronization.

Since most biological, ecological and other physical systems have a complex topology, the study of GS in systems with complex structures became imperative. Coupled units on a network may result in coexisting coherent and incoherent states, namely chimera states that is supported by both theoretical and experimental evidence. This behaviour has been argued to be another manifestation of GS wherein the coherent states are the response units driven by incoherent states.

The phenomenon of GS starting from its introduction has been explored in several scenarios within the realm of dynamical system theory. Strictly speaking, all these discussions have been limited to the case of deterministic systems. Possibility of observing and understanding GS in a stochastic system still remains an open area of research. To generalize the idea of GS in stochastic systems, the auxiliary system approach may not be applicable. It fails in the sense that the response and the auxiliary unit are expected to be in complete synchrony in order for the drive and response to be in GS. Another limitation that one may face is in calculating the LEs for stochastic systems that are expressed in the form of chemical reactions or chemical Langevin equations. Though there are studies that have addressed the issue of GS in this case but a comprehensive study unearthing all the markers that are universal to GS in stochastic systems is required for a better understanding of this phenomenon in its entirety.

Another related idea is the synchronization of chaotic units in the presence of common noise which is a clear example of GS between the noise (drive) and the chaotic units (response). Given the ubiquity of the phenomenon that any natural system is constantly under the influence of noise of varying colours, it becomes important to investigate how the colour of noise influences the nature of synchrony. In general, a natural system may be driven simultaneously by signals of varying nature and hence the very idea of GS when the forcing is in the form of multiple drives that could be a combination of periodic, quasiperiodic, chaotic or noise signals would be a topic of interest to address at a fundamental level.

Furthermore, in the context of complex systems, the interplay of topology and emergence/sustenance of GS can be an interesting possibility to explore in the future.

References

- [1] D Yang, Y Li and A Kuznetsov, *Chaos* **19**, 033115 (2009)
- [2] H Jeong, B Tombor, R Albert, Z N Oltvai and A Barabasi, *Nature (London)* **407**, 651 (2000)
- [3] S Jain and S Krishna, *Proc. Natl. Acad. Sci. USA* **98**, 543 (2001)
- [4] R Albert, I Albert and G L Nakarado, *Phys. Rev. E* **69**, 025103(R) (2004)
- [5] W Willinger, R Govindan, S Jamin, V Paxson and S Shenker, *Proc. Natl. Acad. Sci. USA* **99**, 2573 (2002)
- [6] M E J Newman and J Park, *Phys. Rev. E* **68**, 036122 (2003)
- [7] T Stankovski, T Pereira, P V E McClintock and A Stefanovska, *Rev. Mod. Phys.* **89**, 045001 (2017)
- [8] C Huygens, *Christiaan Huygens' the Pendulum Clock or Geometrical Demonstrations Concerning the Motion of Pendula as Applied to Clocks* (Iowa State University Press, Ames, 1986)
- [9] V S Afraimovich, N N Verichev and M I Rabinovich, *Radiophys. Quantum Electron.* **29**, 795 (1986)
- [10] L Fabiny, P Colet and R Roy, *Phys. Rev. A* **47**, 4287 (1993)
- [11] V S Anisichenko *et al.*, *Int. J. Bifurc. Chaos Appl. Sci. Eng.* **2**, 633 (1992)
- [12] I Schreiber and M Marek, *Physica D* **50**, 258 (1982)
- [13] S K Han, C Kurrer and K Kuramoto, *Phys. Rev. Lett.* **75**, 3190 (1995)
- [14] A Pikovsky, M Rosenblum and J Kurths, *Synchronization. A Universal Concept in Nonlinear Science* (Cambridge University Press, Cambridge, 2001)
- [15] H Fujisaka and T Yamada, *Prog. Theor. Phys.* **69**, 32 (1983)
- [16] L M Pecora and T L Carroll, *Phys. Rev. Lett.* **64**, 821 (1990)
- [17] M G Rosenblum, A S Pikovsky and J Kurths, *Phys. Rev. Lett.* **78**, 4193 (1997)
- [18] M G Rosenblum, A S Pikovsky and J Kurths, *Phys. Rev. Lett.* **76**, 1804 (1996)
- [19] S Guan, C-H Lai and G W Wei, *Phys. Rev. E* **72**, 016205 (2005)
- [20] U Parlitz, L Junge, W Lauterborn and L Kocarev, *Phys. Rev. E* **54**, 2115 (1996)
- [21] Z Zheng and G Hu, *Phys. Rev. E* **62**, 7882 (2000)
- [22] P Perlikowski, A Stefański and T Kapitaniak, *J. Sound Vib.* **318**, 329 (2008)
- [23] L Junge and U Parlitz, *Phys. Rev. E* **62**, 438 (2000)
- [24] M Inoue, T Kawazoe, Y Nishi and M Nagadome, *Phys. Lett. A* **249**, 69 (1998)
- [25] H D I Abarbanel, N F Rulkov and M M Sushchik, *Phys. Rev. E* **53**, 4528 (1996)
- [26] N R Rulkov and M M Sushchik, *Phys. Lett. A* **214**, 145 (1996)
- [27] A Kittel, J Parisi and K Pyragas, *Physica D* **112**, 459 (1998)
- [28] Z Shi-Qun, L Xiao-Qin and F Jian-Xing, *Chin. Phys. Lett.* **18** 727, (2001)
- [29] D Y Tang, R Dykstra, M W Hamilton and N R Heckenberg, *Phys. Rev. E* **57**, 5247 (1998)
- [30] P Parmananda, *Phys. Rev. E* **56**, 1595 (1997)
- [31] J R Terry and G D Van Wiggeren, *Chaos Solitons Fractals* **12**, 145 (2001)
- [32] S S Yang and C K Duan, *Chaos Solitons Fractals* **9**, 1703 (1998)

- [33] T Yang, L-B Yang and C-M Yang, *IEEE* **45**, 1062 (1998)
- [34] D Poland, *Physica D* **65**, 86 (1993)
- [35] N F Rulkov, K M Sushchik, L S Tsimring and H D I Abarbanel, *Phys. Rev. E* **51**, 980 (1995)
- [36] L Kocarev and U Parlitz, *Phys. Rev. Lett.* **76**, 1816 (1996)
- [37] R Brown, *Phys. Rev. Lett.* **81**, 4835 (1998)
- [38] O A Llamoza and M G Cosenza, *Phys. Rev. E* **78**, 046216 (2008)
- [39] M R Molaei and O Umut, *Chaos Solitons Fractals* **37**, 227 (2008)
- [40] S Guan, Y C Lai and C H Lei, *Phys. Rev. E* **73**, 046210 (2006)
- [41] O I Moskalenko and A A Ovchinnikov, *J. Commun. Technol. Electron.* **55**, 407 (2010)
- [42] A E Hramov, A A Koronovskii and O I Moskalenko, *Phys. Lett. A* **354**, 423 (2006)
- [43] A A Koronovskii, O I Moskalenko and A E Hramov, *Tech. Phys. Lett.* **51**, 143 (2006)
- [44] O I Moskalenko, A A Koronovskii and A E Hramov, *Phys. Lett. A* **374**, 2925 (2010)
- [45] A A Koronovskii, O I Moskalenko and A E Hramov, *Tech. Phys.* **55**, 435 (2010)
- [46] A A Ovchinnikov, O I Moskalenko, A A Koronovskii and A E Hramov, *Tech. Phys. Lett.* **36**, 48 (2010)
- [47] H H Jafri, R K B Singh and R Ramaswamy, *Phys. Rev. E* **94**, 055216 (2016)
- [48] D T Gillespie, *J. Chem. Phys.* **113**, 297 (2000)
- [49] D Poland, *Physica D* **65**, 86 (1993)
- [50] A Maritan and J R Banavar, *Phys. Rev. Lett.* **72**, 1451 (1994)
- [51] R Toral, C R Mirasso, E H Garcia and O Piro, *Chaos* **11**, 665 (2001)
- [52] M Lakshmanan and D V Senthilkumar, *Dynamics of Nonlinear Time-Delay Systems* (Springer-Verlag, Berlin, 2011)
- [53] F M Atay, *Complex Time-Delay Systems* (Springer-Verlag, Berlin, 2010)
- [54] H G Schuster and P Wagner, *Prog. Theor. Phys.* **81**, 939 (1989)
- [55] E M Shahverdiev and K A Shore, *Phys. Rev. E* **71**, 016201 (2005)
- [56] X Huang and J Cao, *Nonlinearity* **19**, 2797 (2006)
- [57] D Ghosh, *Nonlinear Dyn.* **59**, 289 (2010)
- [58] D Ghosh, S Banerjee and A R Chowdhury, *Phys. Lett. A* **372**, 2143 (2010)
- [59] D V Senthilkumar and M Lakshmanan, *Phys. Rev. E* **76**, 066210 (2007)
- [60] O I Moskalenko, A A Koronovskii and A E Hramov, *Phys. Rev. E* **87**, 064901 (2013)
- [61] S Guan, C H Lai and G W Wei, *Phys. Rev. E* **71**, 036209 (2005)
- [62] A Bergner, M Frasca, G Sciuto, A Buscarino, E J Ngamga, L Fortuna and J Kurths, *Phys. Rev. E* **85**, 026208 (2012)
- [63] V Vlasov and A Bifone, *Sci. Rep.* **7**, 10403 (2017)
- [64] V Nicosia, M Valencia, M Chavez, A D Guiler and V Latora, *Phys. Rev. Lett.* **110**, 174102 (2013)
- [65] I Fischer, R Vicente, J M Buldu, M Peil, C R Mirasso, M Torrent and J Garcia-Ojalvo, *Phys. Rev. Lett.* **97**, 123902 (2006)
- [66] R Vicente, L L Gollo, C R Mirasso, I Fischer and G Pipa, *Proc. Natl. Acad. Sci.* **105**, 17157 (2008)
- [67] U S Thounaojam and M D Shrimali, *Chaos Solitons Fractals* **107**, 5 (2018)
- [68] R Gutiérrez *et al.*, *Phys. Rev. E* **88**, 052908 (2013)
- [69] C J Stam and B W van Dijk, *Physica D* **163**, 236 (2002)
- [70] J Schumacher, R Haslinger and G Pipa, *Phys. Rev. E* **85**, 056215 (2012)
- [71] K Pyragas, *Nonlinear Analysis: Modelling and Control*, (1998)
- [72] Z Liu and S Chen, *Phys. Rev. E* **56**, 7297 (1997)
- [73] J C Stam, A M van, C van Walsum, A L Y Pijenburg, W H Berendse, J C de Munck, P Scheltens and B W van Dijk, *J. Clinical Neurophysiol.* **19**, 562 (2002)
- [74] L M Pecora, T L Carroll, G A Johnson, D J Mar and J F Heagy, *Chaos* **7**, 1054 (1997)
- [75] U Parlitz and L Junge, *European Control Conference* (1999) pp. 4637–4642
- [76] A E Hramov, A A Koronovskii and P V Popov, *Phys. Rev. E* **72**, 037201 (2005)
- [77] P V Popov, A A Koronovskii and A E Hramov, *Tech. Phys. Lett.* **32**, 638 (2006)
- [78] P V Popov, *Tech. Phys. Lett.* **33**, 788 (2007)
- [79] O I Moskalenko, A A Koronovskii, A E Hramov and S Boccaletti, *Phys. Rev. E* **86**, 036216 (2012)
- [80] H Kato, M C Soriano, E Pereda, I Fischer and C R Mirasso, *Phys. Rev. E* **88**, 062924 (2013)
- [81] A E Hramov and A A Koronovskii, *Europhys. Lett.* **70**, 69 (2005)
- [82] K Pyragas, *Phys. Rev. E* **54**, R4508 (1996)
- [83] T Stankovski, P V E McClintock and A Stefanovska, *Phys. Rev. E* **89**, 062909 (2014)
- [84] Z Liu, *Europhys. Lett.* **68**, 19 (2004)
- [85] H Suetani, Y Iba and K Aihara, *J. Phys. A: Math. Gen.* **39**, 10723 (2006)
- [86] B R Hunt, E Ott and J A Yorke, *Phys. Rev. E* **55**, 4029 (1997)
- [87] L Guo and Z Xu, *Chaos* **18**, 033134 (2008)
- [88] N F Rulkov and V S Afraimovich, *Phys. Rev. E* **67**, 066218 (2003)
- [89] K Pyragas, *Chaos Solitons Fractals* **9**, 337 (1998)
- [90] T U Singh, A Nandi and R Ramaswamy, *Phys. Rev. E* **78**, 025205 (2008)
- [91] T U Singh, H H Jafri and R Ramaswamy, *Phys. Rev. E* **81**, 016208 (2010)
- [92] T U Singh and R Ramaswamy, *NDES2009: The 17th International IEEE Conference Nonlinear Dynamics*

- of *Electronic Systems* (Rapperswil, Switzerland, 21–24 June 2009) (unpublished)
- [93] A Prasad, S S Negi and R Ramaswamy, *Int. J. Bifurc. Chaos* **11**, 291 (2001)
- [94] G Keller, H H Jafri and R Ramaswamy, *Phys. Rev. E* **87**, 042913 (2013)
- [95] L Glass, *Nature* **410**, 277 (2001)
- [96] J L Kaplan and J A Yorke, *Functional Differential Equations and Approximation of Fixed Points*, eds. H-O Peitgen and H-O Walther, *Lecture Notes in Mathematics*, volume 730 (Springer-Verlag, Berlin, 1979) p. 204
- [97] J-P Eckmann, S O Kamphorst, D Ruelle and S Ciliberto, *Phys. Rev. A* **34**, 4971 (1986)
- [98] K Pyragas, *Phys. Rev. E* **56**, 5183 (1997)
- [99] D He, Z Zheng and L Stone, *Phys. Rev. E* **67**, 026223 (2003)
- [100] V Afraimovich, J R Chazottes and A Cordonet, *Discrete Contin. Dyn. Syst., Ser. B* **1**, 421 (2001)
- [101] K Manchanda and R Ramaswamy, *Phys. Rev. E* **83**, 066201 (2011)
- [102] J Yang and G Hu, *Phys. Lett. A* **361**, 332 (2007)
- [103] A H Hu, Z Y Xu and L X Guo, *Nonlin. Anal.: Theory, Methods Appl.* **71**, 5994 (2009)
- [104] A Hu, Z Xu and L Guo, *Phys. Lett. A* **373**, 2319 (2009)
- [105] A Barabasi and M Posfai, *Network Science* (Cambridge University Press, Cambridge, 2016)
- [106] D R Chialvo, *Nat. Phys.* **6**, 744 (2010)
- [107] L V Gambuzza, M Frasca, L Fortuna and S Boccaletti, *Phys. Rev. E* **93**, 042203 (2016)
- [108] L Zhang, A E Motter and T Nishikawa, *Phys. Rev. Lett.* **118**, 174102 (2017)
- [109] Y C Hung, Y T Huang, M C Ho and C K Hu, *Phys. Rev. E* **77**, 016202 (2008)
- [110] S Guan, X Wang, X Gong, K Li and C-H Lai, *Chaos* **19**, 013130 (2009)
- [111] A Hu, Z Xu and L Guo, *Chaos* **20**, 013112 (2010)
- [112] J Chen, J Lu, X Wu and W X Zheng, *Chaos* **19**, 043119 (2009)
- [113] Y Shang, M Chen and J Kurths, *Phys. Rev. E* **80**, 027201 (2009)
- [114] X Xua, Z Chen, G Si, X Hu and P Luo, *Comput. Math. Appl.* **56**, 2789 (2008)
- [115] H Liu, J Chen, J Lu and M Cao, *Physica A* **389**, 1759 (2010)
- [116] A A Koronovskii, O I Moskalenko and A E Hramov, *Tech. Phys. Lett.* **38**, 924 (2012)
- [117] Y Kuramoto and D Battogtokh, *Nonlin. Phenom. Complex Syst.* **5**, 380 (2002)
- [118] M J Panaggio and D M Abrams, *Nonlinearity* **28**, R67 (2015)
- [119] R G Andrzejak, G Ruzzene and I Malvestio, *Chaos* **27**, 053114 (2017)
- [120] X Zhang, H Bi, S Guan, J Liu and Z Liu, *Phys. Rev. E* **94**, 012204 (2016)
- [121] A E Botha and M R Kolahchi, *Sci. Rep.* **8**, 1830 (2018)
- [122] E A Martens, S Thutupalli, A Fourrière and O Hallatscheka, *Proc. Natl. Acad. Sci. USA* **110**, 0563 (2013)
- [123] D M Abrams and S H Strogatz, *Phys. Rev. Lett.* **93**, 174102 (2004)
- [124] A E Botha, *Sci. Rep.* **6**, 29213 (2016)
- [125] B S Dmitriev, A E Hramov, A A Koronovskii, A V Starodubov, D I Trubetskov and Y D Zharkov, *Phys. Rev. Lett.* **102**, 074101 (2009)
- [126] A V Starodubov, A A Koronovskii, A E Khramov, Y D Zharkhov, B S Dmitriev and V N Skorokhodov, *Phys. Wave Phen.* **18**, 51 (2010)
- [127] Y L Feng, X H Zhang, Z G Jiang and K Shen, *Int. J. Mod. Phys. B* **24**, (5)675 (2010)
- [128] D Y Tang, R Dykstra, M W Hamilton and N R Heckenberg, *Phys. Rev. E* **57**, 5247 (1998)
- [129] S Chishti and R Ramaswamy, *Phys. Rev. E* **98**, 032217 (2018)
- [130] T Stankovski, T Pereira, P V E McClintock and A Stefanovska, *Rev. Mod. Phys.* **89**, 045001 (2017)
- [131] X Wang and X Gong, *Chaos* **15**, 023109 (2005)
- [132] R Mainieri and J Rehacek, *Phys. Rev. Lett.* **82**, 3042 (1999)
- [133] G Álvarez, S Li, F Montoya, G Pastor and M Romera, *Chaos Solitons Fractals* **24**, 775 (2005)
- [134] R Femat, L Kocarev, L V Gerven and M E Monsivais-Pérez, *Phys. Lett. A* **342**, 247 (2005)
- [135] R Varshney and H H Jafri, Manuscript in preparation.
- [136] U Parlitz, L Junge and L Kocarev *Phys. Rev. Lett.* **79**, 3158 (1997)
- [137] E Barreto, P So, B J Gluckman and S J Schiff, *Phys. Rev. Lett.* **84**, 1689 (2000)
- [138] N F Rulkov and C T Lewis, *Phys. Rev. E* **63**, 065204(R) (2001)
- [139] G B Mindlin, H G Solari, M A Natiello, R Gilmore and X J Hou, *J. Nonlinear Sci.* **1**, 147 (1991)
- [140] S Guang, C H Lai and G W Wei, *Phys. Rev. E* **72**, 016205 (2005)